JOURNAL OF COLLOID AND INTERFACE SCIENCE 161, 335–342 (1993)

Dynamic Considerations in the Closing and Opening of Holes in Thin Liquid Films

J. A. MORIARTY*,[1] AND L. W. SCHWARTZ†,[2]

*Department of Mechanical Engineering, University of Delaware, Newark, Delaware 19716; and †Departments of Mechanical Engineering and Mathematical Sciences, University of Delaware, Newark, Delaware 19716

Received March 12, 1993; accepted July 15, 1993

Whether holes in thin films close or open is an important issue in the design of liquid coatings. Previous analyses, for example the work of Taylor and Michael (*J. Fluid Mech.* 58, 625 (1973)) predict a static criterion for hole closure based on a balance between capillary and gravitational forces. In the present work we develop a numerical model which follows the evolution of holes to determine whether they close or open. The model is based on the lubrication approximations and requires input of the advancing and receding contact angles. Because viscous forces are also included in the present model, the static criteria can be reevaluated using the more complete theory. We find that holes which the static criteria predict will close can actually open, and vice versa.

1. INTRODUCTION

In the coating industry, the thickness of the coating to be applied very often involves a trade-off between expense of application and uniformity of the final coating film. The thicker the coating, the more material and time are required in the application process, and hence the greater the cost. On the other hand, the coating should not be so thin that the coating layer fails, forming holes and other irregularities. Nonuniform films are not only aesthetically displeasing, but, in many cases, are totally unacceptable. This is especially true when the coatings are applied for protective purposes.

As the thickness of the coating film decreases, the film becomes more sensitive to outside disturbances, and holes often form. The reasons for hole formation are many and varied. Air bubbles entrapped in the coating fluid, which may have formed, for example, during the stirring process, can burst once the film has been applied, forming holes which may never heal. In air spraying, the impacting droplets of paint can often create holes in the applied film (2).

Holes can also occur due to inhomogeneities in the solid substrate to be coated. For example, if the substrate has contaminated patches with lower surface energy than the rest of the solid, in many cases it will be energetically less expensive for the coating fluid to stretch around the patch, leaving a dry area. Depending on the surface energies of the liquid and solid substrate, and on the fluid viscosity, this dry patch may remain so.

Another mechanism for hole formation arises due to the presence of surfactants in the paint. These surfactants generally have lower surface energies and thus tend to spread along the fluid interface. Since the bulk of the fluid moves with the surface layer, craters are often formed (2). If the crater becomes so deep that the surfactant contacts the solid surface, forming a contaminated region there, the applied film may never be restored to its uniform configuration.

The fluid dynamics of film rupture, associated with disjoining pressure, has been treated by Burelbach *et al.* (3) and represents another mechanism for the formation of holes in thin liquid films. In this paper, we focus on the fate of holes once they have been formed, in order to understand how the holes are affected by film thickness and a host of other parameters. This issue is especially relevant to the coatings industry. At the very least, if one accepts that holes will inevitably form in all coating layers, a study of these systems will provide the industry with a lower bound for the coating thickness required to ensure hole "filling."

Strangely enough, however, the issue of hole closure has been touched very little by the scientific community. In 1954, Dombrowski and Frazer (4), in an experimental study into the disintegration of fluid sheets, showed that large holes expanded outward, while small holes closed. Padday (5) extended their experimental work to determine the critical rupture thicknesses of other fluid/solid systems.

In 1973, Taylor and Michael (T&M) (1) conducted a stability study of holes in horizontal sheets of fluids to determine a criterion for when holes open, and one for when they close. In doing so, they solved the static capillarity–gravity equation for holes in thin sheets of fluid of infinite extent. For a given fluid depth and contact angle, a unique solution exists for this equation, which T&M showed to rep-

[1] Present address: Mathematical Institute, 24-29 St. Giles', Oxford, OX1 3LB United Kingdom.

[2] To whom correspondence should be addressed.

0021-9797/93 $5.00

resent an unstable equilibrium position; holes of size greater than the unstable size open, and those of smaller size close.

In a recent paper by Sharma and Ruckenstein (S&R)(6), the energetics of hole formation were considered. In their work, the energy of the hole profile relative to the undisturbed uniform film, which they called the free energy ΔF, was used as a measure of the energy of the system. They denoted the hole radius at which the free energy of the system is zero as the critical radius and the radius of the unstable equilibrium configuration as the transitional radius. They were in agreement with T&M that holes smaller than the transitional radius closed, but argued that holes of size larger than the transitional hole size but less than the critical hole size do not necessarily open but can either close or open out. Their arguments for this are purely qualitative and are based on energy considerations.

In this paper, we look at axisymmetric holes in sheets of fluid of finite extent, for example, holes bounded by rigid, vertical side walls. Because the films are thin, with the contact angle ϕ being much less than 90°, the lubrication approximations may be used to study such systems. The equilibrium positions are determined by solving the static-capillarity equation for thin films of finite extent. Unlike for the infinite film case, the static-capillarity equation now yields two equilibrium solutions: the unstable equilibrium solution and a stable solution, where the fluid piles up around the outer rim of the bounded domain.

We develop a numerical algorithm to solve the unsteady problem; it is used to march the hole profiles in time, thus following the evolution of the holes to determine whether they open or close. In using such an approach, the fluid dynamics of the system is incorporated into the analysis, a feature lacking in the static analyses of T&M and S&R. For example, a study of the time-dependent problem can incorporate the phenomenon of contact angle hysteresis. The program has the ability to wet and de-wet the surface, and we find that the hole profiles either close to form a uniform liquid film configuration or open up until the stable equilibrium position is attained. Whether the profiles actually open, or close, is dependent upon the initial profile configuration, and not just on the hole size; we show that some holes open when T&M say they close, and vice versa.

2. EQUILIBRIUM SOLUTIONS

A cross-section of the hole profile considered in the present work is shown in Fig. 1. The hole, of radius R, is axisymmetric around its center $r = 0$, and bounded by a rigid vertical wall at $r = L$. The fluid surface is given by $h(r, t)$. The fluid has surface tension σ and meets the horizontal substrate with contact angle ϕ. The fluid density is ρ and gravity g acts downward. The air/substrate and fluid/substrate interfacial surface tensions are given by γ_{sv} and γ_{sl}, respectively.

For the liquid to be in static equilibrium, the pressure

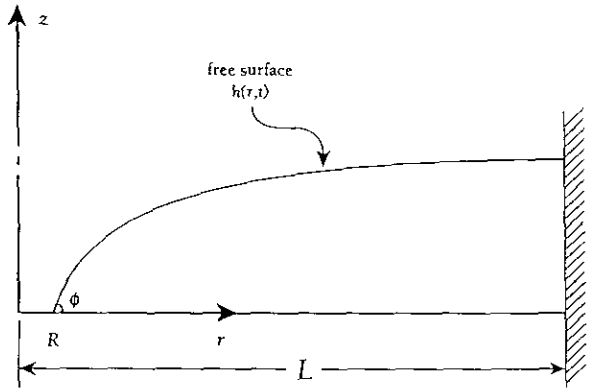

FIG. 1. Cross-section of the hole profile.

distribution within it must be hydrostatic. This leads to the equation

$$\sigma\kappa = \rho g h + p_0, \qquad [2.1]$$

where κ is the mean curvature of the profile and p_0 is an arbitrary constant. This equation can also be obtained by minimizing the energy of the system.

For thin films, where the small slope approximation applies, which is the case for sufficiently small contact angles, the curvature is approximately given by

$$\kappa \approx \nabla^2 h = \frac{1}{r}\frac{\partial}{\partial r}\left(r\frac{\partial h}{\partial r}\right), \qquad [2.2]$$

so that [2.1] becomes

$$\sigma\frac{1}{r}\frac{\partial}{\partial r}\left(r\frac{\partial h}{\partial r}\right) - \rho g h = p_0, \qquad [2.3]$$

with boundary conditions

$$h(R) = 0, \qquad [2.4]$$

$$h'(R) = \tan\phi. \qquad [2.5]$$

The arbitrary constant p_0 is determined by prescribing the additional condition that $h'(L) = 0$.

Scaling r and h by the capillary length $a = \sqrt{\sigma/\rho g}$ renders [2.3]–[2.5] nondimensional and yields the solution in terms of modified Bessel functions,

$$h = A[I_0(r) - I_0(R)] + B[K_0(r) - K_0(R)], \qquad [2.6]$$

where

$$A = \frac{K_1(L)\tan(\phi)}{K_1(L)I_1(R) - K_1(R)I_1(L)} \qquad [2.7]$$

and

$$B = \frac{I_1(L)\tan(\phi)}{K_1(L)I_1(R) - K_1(R)I_1(L)}. \qquad [2.8]$$

For a given contact angle ϕ and hole radius $R < L$, the liquid volume in the cylindrical region may be calculated. Results are shown in Fig. 2 for $L = 5$ and several contact angles. We note that there are two distinct equilibrium solutions, with different hole radii, for each liquid volume. There is also a maximum fluid volume, above which no equilibrium solution exists. Subsequently it will be demonstrated that the fluid shape corresponding to the smaller hole radius is unstable, while that for the larger hole radius is stable.

The maximum volume, for given ϕ and L, suggests that there is a critical volume of liquid $V^*(\phi, L)$ for which all holes close, according to the static analysis. Figure 2 indicates that for $\phi = 0.5$, V^* is approximately equal to $4(2\pi a^3)$ in dimensional units. The corresponding critical average depth is $h^* = V^*/\pi L^2 = 0.32a$. This may be compared to a result of Lamb (7) who solved the exact Young–Laplace equation [2.1] for a liquid film of infinite extent. His result is $h^*_\infty = 2a \sin(\phi/2)$. The small slope version of this result, which may be obtained from Eq. [2.6] in the limit as $L \to \infty$, is $h^*_\infty = a \tan \phi$, the difference between the two estimates being of order ϕ^3. For example, for a contact angle of 0.5, Lamb's value for h^*_∞ is about $0.495a$, while the small slope approximation is about 10% higher. In either event, the infinite film analysis significantly overpredicts the critical depth necessary to ensure coverage in the present case.[3]

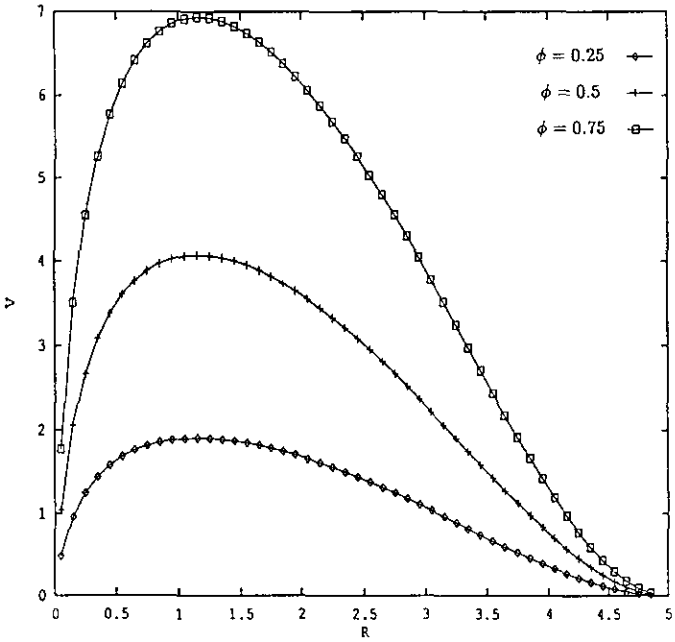

FIG. 2. Volume V of fluid vs hole radius R for some equilibrium configurations with given contact angle ϕ.

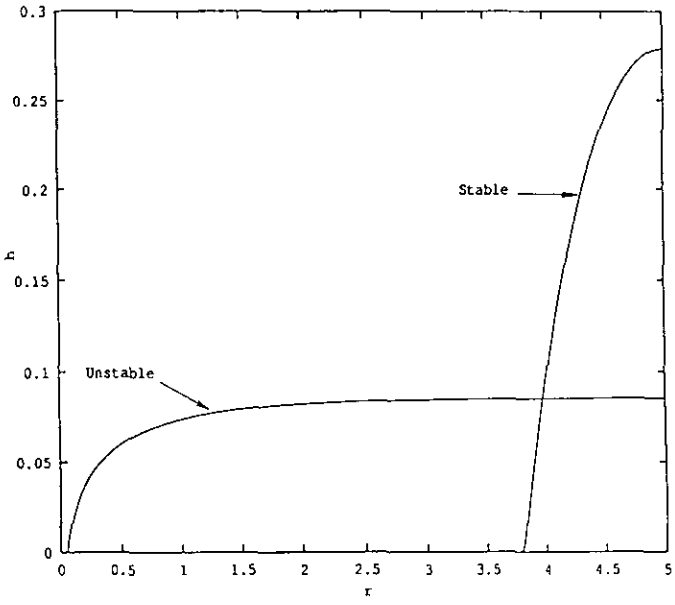

FIG. 3. An example of an unstable hole configuration ($R_0 = 0.05$) and its stable counterpart ($R_0 = 3.8$). The contact angle is $\phi = 0.5$.

Two representative equilibrium configurations, corresponding to the same liquid volume and contact angle, are shown in Fig. 3.

3. TIME EVOLUTION OF HOLE FORMATION/DEFORMATION

The evolution equation for the time-dependent motion of hole formation/deformation is derived from the simplified Navier–Stokes equations. For thin films where the flow is approximately unidirectional in the radial direction, the radially directed nondimensional Navier–Stokes equation is

$$\frac{\partial^2 u}{\partial z^2} = -p_r, \qquad [3.1]$$

where u is the radially directed velocity and p_r is the nondimensional pressure gradient. Validity of [3.1] relies on the assumption that $(\rho U a/\mu)(h_\infty/a)^2$ is much less than unity, where U is some characteristic velocity. Since the films are typically thin and slowly moving, this condition is generally satisfied.

[3] In fact, the reason for this is clear. The difference between the two cases is the boundary condition or contact angle on the side walls. If the same small contact-angle condition had been imposed there, the critical thickness required for guaranteed coverage would greatly exceed h^*_∞ since a significant fluid volume would then be relegated to the meniscus region and would not be available for uniform coverage. Thus, the infinite film predictions of Lamb will not, in general, be particularly useful for bounded regions, unless they are quite large.

We assume zero shear stress at the free surface and no slip on the horizontal substrate. This latter condition is a controversial one, however. Since the requirement of no slip is in direct opposition to the requirement for contact-line movement, this gives rise to a nonintegrable stress singularity within the continuum theory. Our justification for imposing no slip, and thereby ignoring the singularity, lies in the fact that we solve the governing equation numerically. We argue that slip is implicitly built into the numerical scheme through the finite grid spacing, and thus need not be imposed explicitly through the boundary conditions.

Grounds for such an argument lie in work done by the authors in a previous paper (8). In that paper, we solved the lubrication equation for a two-dimensional drop draining under gravity down a dry vertical wall. We used two models, one which relaxed the no-slip condition at the moving contact line and one which did not. The model with slip was based on Greenspan's slip model (9), although the same analysis could be extended to other slip models.

For the model without slip, the numerical scheme did not converge under spatial refinement. This was a numerical manifestation of the stress singularity. The model with slip was convergent. We showed that, for a given value of the grid spacing in the no-slip model and a given slip length (effectively the length over which the no-slip condition is relaxed) in the slip model, both models gave exactly the same solution for the free-surface profiles. We thus concluded that numerical grid spacing and slip are equivalent.

The computations described in the present work utilize a uniform gridspacing of 0.05. Based on results of the previous paper, such a grid spacing corresponds to an effective slip length, α, in Greenspan's slip model, of about 0.005.

At the present time, however, this effective slip length is still an unknown quantity. Thus, the equivalent value of grid spacing is not uniquely specified by the problem, but is a free parameter to be assigned.

Neogi and Miller (10) have argued that this slip length can be related to surface porosity and roughness. This argument is substantiated by the recent work of Dussan *et al.* (11), which indicates that this slip length is a material property of the liquid/substrate system and so would differ from one system to another. Thus, whatever reasonable slip length is assigned in the present work, it is valid for some system, though lack of experimental data prohibits us from specifying exactly which one at the present time.

Since the films are thin, we assume the pressure is constant across the layer, in accordance with lubrication theory, so that p_r is given by

$$p_r = \frac{\partial}{\partial r}\left[\frac{1}{r}\frac{\partial}{\partial r}\left(r\frac{\partial h}{\partial r}\right)\right] - \frac{\partial h}{\partial r}. \qquad [3.2]$$

The first term on the right-hand side is the surface tension contribution and the second term is the hydrostatic contribution. Note that p scales with σ/a, and t with $3\mu a/\sigma$ so that the viscosity appears only in the time scaling.

Substituting [3.2] into [3.1], then integrating, using the boundary conditions of zero shear stress at the free surface and the no-slip condition on the solid substrate, gives

$$u = -p_r\left[\frac{z^2 - 2hz}{2}\right]. \qquad [3.3]$$

The radially directed flux,

$$q = \int_0^h u dz = \frac{p_r h^3}{3}, \qquad [3.4]$$

and conservation of mass,

$$\frac{\partial h}{\partial t} = -\frac{1}{r}\frac{\partial (rq)}{\partial r}, \qquad [3.5]$$

then give the evolution equation

$$\frac{\partial h}{\partial t} = -\frac{1}{r}\frac{\partial}{\partial r}\left[rh^3\left(\frac{\partial}{\partial r}\left(\frac{1}{r}\frac{\partial}{\partial r}\left(r\frac{\partial h}{\partial r}\right)\right) - \frac{\partial h}{\partial r}\right)\right]. \qquad [3.6]$$

The boundary conditions are

$$h(R) = 0, \qquad [3.7]$$

$$h'(R) = \tan\phi, \qquad [3.8]$$

$$h'(L) = 0, \qquad [3.9]$$

and

$$q(L) = 0. \qquad [3.10]$$

The initial condition $h(r, 0)$ is a prescribed initial profile. Since h and r are both scaled with the capillary length, the contact angle is the same in both dimensional and nondimensional units. The model assumes that the fluid propagates with a contact angle equal in value to the static advancing or receding contact angle.[4]

This equation is solved using a finite difference time-marching scheme which solves for the profile $h(r, t)$ as it evolves. The advancing contact angle ϕ_A and the receding contact angle ϕ_R, such that $\phi_R < \phi < \phi_A$, are imposed by not letting the profile move forward or backward, respectively, until these angles are reached. This difference allows the profile to attain a *range* of equilibrium states which encompasses all steady-state profiles with contact angles satisfying $\phi_R < \phi < \phi_A$. In this sense, the dynamic study can model the phenomenon of contact-angle hysteresis—something a static analysis can not do.

[4] This is a controversial issue in itself: for a more detailed discussion on the topic, see Moriarty (12).

The fluid recedes by "dewetting" from the solid surface. Details of the numerical scheme, as well as details on how dewetting is achieved computationally, will be given in the following section.

For any given hole profile $h(r, 0)$, we then follow its evolution, thus determining whether the hole closes to form the uniform thin-film configuration or opens out to the stable equilibrium configuration. For some given profiles $h(r, 0)$, we show that the T&M criterion is inadequate in predicting whether holes open outward or not.

In order to model realistic holes, we create holes by mathematically modeling the blowing of a jet of air down onto the center of a thin axisymmetric film. This is achieved computationally by imposing a gaussian pressure distribution on the film (13). The thickness of the film decreases and, when it gets below a certain prescribed minimum thickness, we assume that the film has ruptured and the hole has been created.

When the hole size is close to, but larger than, the unstable hole size R_l, the hole can either close in or open outward, and our computations show this. This sort of situation is predicted by S&R. S&R predict this behavior for a range of hole sizes having a radius larger than the unstable hole size. We find that this range of hole sizes is generally narrow and that the fate of most realistic holes of size larger than the unstable hole size is one of hole opening, as predicted by T&M.

3.1. *The Computational Model*

3.1a. The finite-difference scheme. In order to formulate the numerical scheme, the flow domain is discretized into n cells and low-order central differences are employed to evaluate the depth of fluid $z = h(r, t)$ at the midpoint of these cells, with fluxes being computed at cell boundaries. Mass is strictly conserved by demanding

$$h(i)^{k+1} = h(i)^k - \frac{\Delta t}{\Delta x}\frac{1}{r(i)}[r(i+1/2)q(i) - r(i-1/2)q(i-1)], \quad [3.11]$$

where $q(i)$ is the flux between the ith and $i+1$th nodal points, and the k superscript indicates the kth time level.

The solution is marched in time using a partially implicit Crank–Nicolson-type method, so that the evaluation of $h(i)$ at the $(k+1)$th time step is obtained according to the numerical scheme

$$h(i)^{k+1} + \frac{\Delta t}{2r(i)\Delta r}[r(i+1/2)q(i)^{k+1} - r(i-1/2)q(i-1)^{k+1}] = h(i)^k - \frac{\Delta t}{2r(i)\Delta r} \times [r(i+1/2)q(i)^k - r(i-1/2)q(i-1)^k], \quad [3.12]$$

where, if $r(i) = (i - 0.5)\Delta r$, then

$$q(i)^k = \left[\left(\frac{h(i)^k + h(i+1)^k}{2}\right)\right] \times \left[\frac{ih(i)^k - (2i+1)h(i+1)^k + (i+1)h(i+2)^k}{(i+0.5)\Delta r^3} - \frac{(i-1)h(i-1)^k - (2i-1)h(i)^k + ih(i+1)^k}{(i-0.5)\Delta r^3} - \frac{h(i+1)^k - h(i)^k}{\Delta r}\right]. \quad [3.13]$$

Note that the nonlinear h^3 term is always evaluated at the previous k time level.

The contact line is at $i = i_{\text{start}} - \frac{1}{2}$. At the $i = i_{\text{start}}$ grid point, the higher derivative is evaluated using $h(i_{\text{start}})$, $h(i_{\text{start}} + 1)$, and $h'(i_{\text{start}} - \frac{1}{2})$, where $h'(i_{\text{start}} - \frac{1}{2}) = \tan\phi$.

The numerical scheme at the contact line is illustrated in Fig. 4.

3.1b. Advancing and receding the contact line. For the profile to either advance or recede, we prescribe the advancing contact angle, ϕ_A, and the receding contact angle, ϕ_R, where $\phi_R < \phi < \phi_A$. The contact line advances by taking $q(i_{\text{start}} - 1) = 0$ unless the numerical contact angle (that angle based on numerical computations at the contact line) is exceeded. This translates to

$$q(i_{\text{start}} - 1) = 0 \quad \text{when} \quad \frac{2h(i_{\text{start}})}{\Delta r} < \tan\phi_A. \quad [3.14]$$

If the numerical contact angle $2h(i_{\text{start}})/\Delta r$ exceeds the advancing contact angle, then the contact line is advanced by decrementing i_{start} by one grid point, so that the new contact line is at $i_{\text{start}} = i_{\text{start}} - 1$. If $i_{\text{start}} = 1$, the hole has closed and the boundary conditions change to symmetry boundary conditions, i.e., $q(i-1) = 0$ and $\partial h/\partial r = 0$.

The receding contact line has a similar criterion and recedes (or dewets) when

$$\frac{2h(i)}{\Delta r} < \tan\phi_R. \quad [3.15]$$

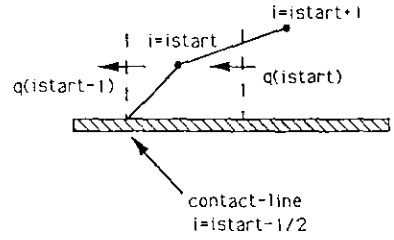

FIG. 4. The numerical scheme at the contact line of a rim of fluid enclosing a circular hole.

The contact line is receded by incrementing it by one grid point. such that $i_{start} = i_{start} + 1$. In addition, the old $h(i_{start})$ is set to zero. In order to conserve volume, the new $h(i_{start})$ must be changed accordingly. Thus, before receding the contact line, we set

$$h(i_{start} + 1) = h(i_{start} + 1) + h(i_{start}) \frac{r(i_{start})}{r(i_{start} + 1)}, \quad [3.16]$$

and then

$$h(i_{start}) = 0. \quad [3.17]$$

Finally, we can recede the contact line so that the new i_{start} is at $i_{start} = i_{start} + 1$.

At times shortly after the contact line recedes, the numerical contact angle may be (falsely) greater than the advancing contact angle. If the contact line is allowed to advance in response to this, the new numerical contact angle will be less than the receding angle, and so it will recede, and the process will repeat itself. Thus, the contact line will tend to oscillate back and forth between the advancing and receding modes. Of course, this situation would not arise in reality and is really just a manifestation of the artificial way in which the contact line is advanced and receded.

One way of circumventing this problem is to set a computational flag, which allows the computer to discern between when the contact line is physically advancing, or receding, and when its tendency toward movement is solely artificial. We thus enforce that the contact line is advanced when $\partial h(i_{start})^{k+1}/\partial r > \partial h(i_{start})^{k}/\partial r$. The converse holds for the receding case.

4. STABILITY STUDY

The time-dependent program provides us with a vehicle by which to conduct a stability study of the equilibrium profiles. By perturbing the profiles so that $R = R_0 \pm \delta$, where R_0 is the radius of the equilibrium configuration and δ is a small number, we can follow the evolution of the profiles to determine whether they are stable or unstable. If the profiles return to their initial states, they are stable. Justification in drawing such a conclusion is that the nonlinearity of the governing equation, as well as "noise" implicit to numerical calculations, entails that the perturbation encompasses all modes of instabilities. On the other hand, if a small perturbation initiates gross movement, we can conclude that the hole configuration is unstable. The rate at which the perturbed profile returns, or diverges, from its initial position gives an indication as to how stable or unstable a particular configuration is.

We consider the case when the contact angle is $\phi = 0.5$. Figure 2 indicates that the critical volume above which all holes close is $V^* \approx 4$ in dimensionless units. At this volume, the hole radius is $R_0 \approx 1.2$.

We perturb those profiles which lie on the curve to the left of the critical volume. Perturbing, so that $R = R_0 - \delta$, we find that all of the holes close, thus indicating that these equilibrium configurations are unstable. These are the hole configurations analyzed by T&M and S&R in their work on holes in infinite sheets of fluid and we confirm their conclusion. In doing so, we confirm our suspicion that the smaller hole in Fig. 3 is unstable.

Perturbing these unstable holes to the right, such that $R = R_0 + \delta$, produces various outcomes, depending on the volume of the fluid. When the hole configuration, with $V \approx 1$ ($R_0 = 0.05$), is perturbed to the right, the hole immediately seeks its secondary equilibrium solution, at $R_0 = 3.8$. For these thin films, the stabilizing gravitational force is negligible and the fluid predominantly wants to minimize surface energy. It does this by reducing its surface area and retracting to its secondary equilibrium position. The speed at which the hole retracts to the secondary equilibrium configuration indicates that its first configuration is a highly unstable one.

For thicker films, a much larger perturbation is required to cause a hole to move toward its secondary equilibrium position. The gravitational energy is minimized by hole closure and this counteracts the tendency of the profile to minimize its surface energy by opening. Often the perturbation is quickly damped and the system attains a steady-state configuration lying within the contact-angle hysteresis range.

The right-hand side of the V vs R curve in Fig. 2, where $R > 1.2$, corresponds to the larger hole configuration of the two equilibrium solutions. Perturbing, so that $R = R_0 - \delta$, shows that thicker films tend to stabilize and attain an equilibrium position lying within the contact-angle hysteresis range. On the other hand, for thinner films, there is a relatively large restoring force due to surface energy minimization which causes the holes to recover their initial position immediately, even after the slightest perturbation. The fact that these larger holes return to their original positions subsequent to a perturbation indicates that they are stable, thus confirming our suspicion that the larger hole configuration in Fig. 3 is indeed stable.

Figure 5 gives a summary of the stability analysis.

5. SOME COMPUTATIONS

In order to create a realistic hole computationally, we have developed a numerical scheme to mathematically model a jet of air blowing down on a thin film. The hole is created when the thickness of the film becomes less than some critical thickness. Once these holes are created, the computational model, described in Section 3, is used to calculate their evolution in time.

Computations are based on a static contact angle of $\phi = 0.5$ and advancing and receding contact angles of 0.55 and

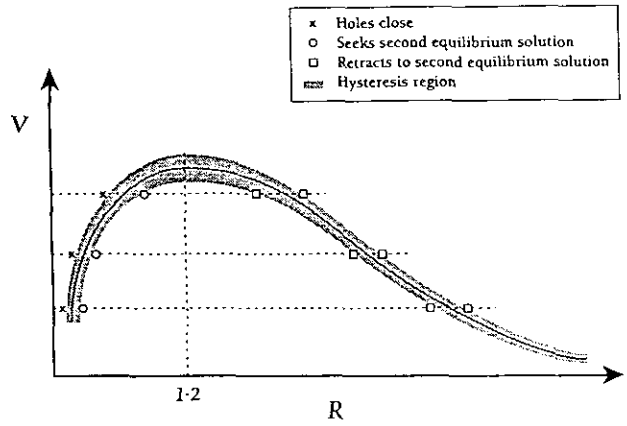

FIG. 5. Results of the stability study.

0.45, respectively. Results have shown that there is a region encompassing hole sizes just greater than the transitional (unstable) hole size, in which these holes can either close or open. Generally this region is narrow. Some of these holes have enough energy to negotiate the energy maximum and actually close. Figure 6 shows a pressure-generated hole which T&M say should open out and yet actually closes. Figure 7 shows a pressure-generated hole which is of the same size as the hole in Fig. 6 but with a slightly lower surface energy. The hole starts to close, then finds it does not have enough energy to do so and actually opens outward to the stable-hole configuration.

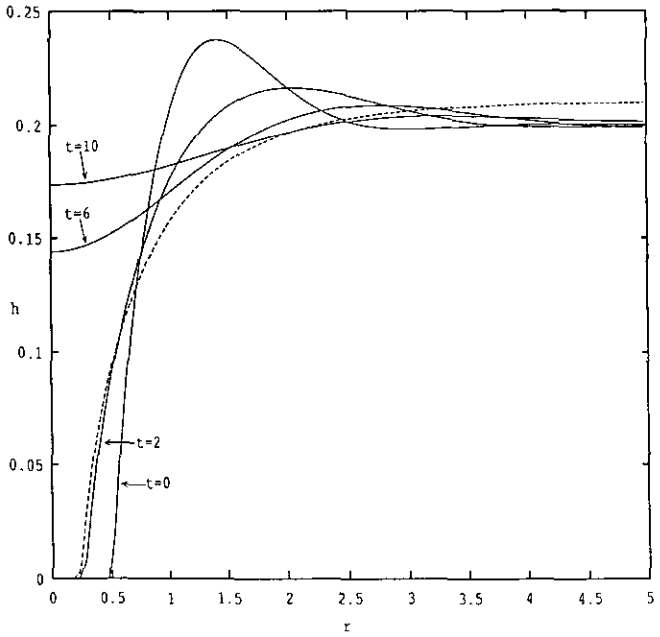

FIG. 6. A realistic hole with radius larger than the transitional radius, which closes. T&M's analysis predicts the hole opens. The dashed line is the unstable equilibrium solution.

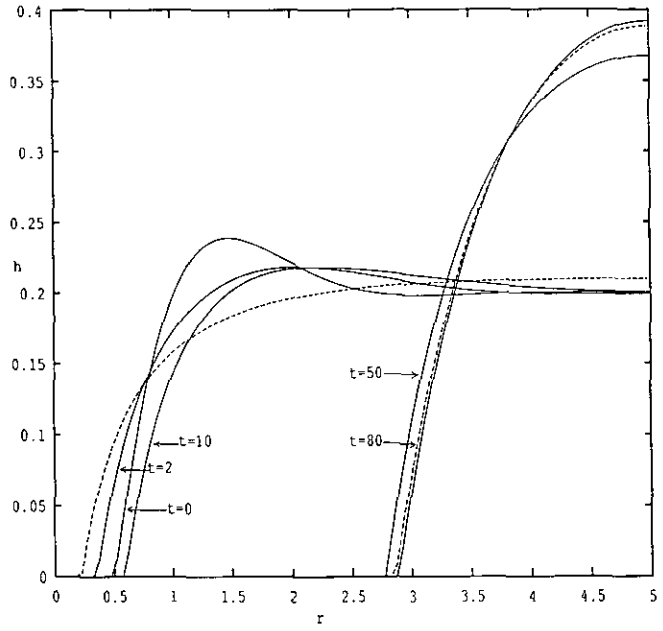

FIG. 7. The same hole size as that in Fig. 6, but with a slightly lower local energy initially. The energy of the initial profile is larger than the energy of a uniform film, yet the hole opens outward. The dashed lines represent the equilibrium solutions.

Contact-line motion, and the magnitude of the viscous dissipation associated with it, is a function of the amount of slip allowed in the model. The effective slip coefficient can be made smaller by about a factor of four by halving the gridspacing (8). We have repeated the calculations for the holes shown in Figs. 6 and 7 for a grid spacing of $\Delta x = 0.025$. In this case, there was enhanced viscous dissipation and this detracted from the free energy of the system, so that the hole of Fig. 6 no longer had enough energy to close. The advancing contact angle for this hole was then decreased by 0.08 and the hole had enough energy to close. From this we conclude that the issue of hole closure/opening is dependent on the amount of slip. As discussed earlier, however, this parameter is a property of the fluid/substrate system and is unknown at the present time.

Figure 8 represents the time evolution of the free energy ΔF, i.e., the energy of the system relative to the uniform film configuration, of the hole in Fig. 7 as it closes. It can be seen that the profile always evolves in the direction of minimum energy. It is interesting to note that the hole dewets before its free energy becomes negative.

6. CONCLUSIONS

In this paper, we have developed a tool to perform time-dependent calculations of holes closing and opening. This tool has benefits that the static analysis could not provide, since it can take into account the characteristics of the film profile on a local scale. For example, external vibrations can

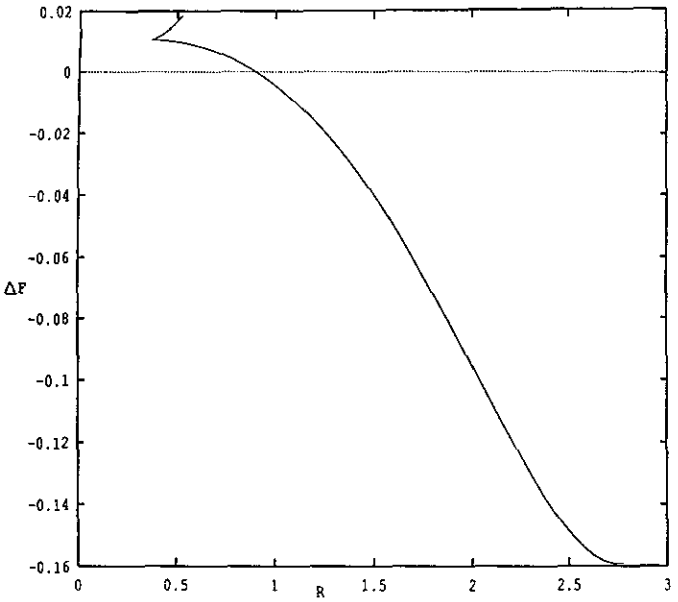

FIG. 8. Evolution of the free energy ΔF (with respect to the uniform film configuration) of the hole in Fig. 7, with the size of the hole R.

give rise to local energy densities in the film profile, which would provide the hole with enough energy to close. Since the static analyses depend only on the hole size, film depth, and static contact angle, they could not take into account such local behavior and can only provide predictions in a more global sense.

The present analysis also has the ability to handle the complex phenomenon of contact-angle hysteresis. The best that the static analysis can do in handling this phenomenon is to define a range of configurations, $\phi_R < \phi < \phi_A$, in which the holes can either close inwards or open outward. As has been demonstrated, the time-dependent calculations can actually determine the fate of all holes lying in this region definitively.

The stability study is greatly simplified by using a time-dependent scheme to follow the subsequent evolution of a hole profile once it has had some perturbation imparted to it. The relative rate at which the profile responds to a perturbation gives an indication of the magnitude of the instability of the profile. For example, our stability study shows that holes in thin fluids are highly unstable.

In order to study the behavior of realistic holes, we have developed a computational model of a jet to create holes in sheets of fluids. Results have shown that the static criterion for holes closing and opening is quite good, except for holes of size just greater than the transitional hole size. In this region, holes can either close or open, as predicted by S&R. Generally speaking the closer the hole is to the transitional hole radius, the more probable it is the hole will close. However, depending on the surface energy of the film profile, some larger holes may close, while the smaller ones open. Since local energy densities are quickly damped, this region of "metastability" is generally narrow and we find that most holes do actually obey the capillary-statics criterion of T&M.

Incorporating different flow rheologies, for example non-Newtonian fluids, as well as the presence of surfactants, lies within the capabilities of the numerical scheme.

Because this problem involves the movement of a fluid within two well-defined configurations, it lends itself very well to a study of the dependency of the boundary conditions imposed at the contact line and the rate of contact-line propagation. For example, the time it takes for a well-defined hole to close could easily be measured experimentally. How well the experimental time matches that determined by the time-marching scheme could be used as a datum to gauge the accuracy of different contact-line boundary conditions. This is a large and complicated study, however, and is beyond the scope of the present work.

REFERENCES

1. Taylor, G. I., and Michael, E., *J. Fluid Mech.* **58,** 625 (1973).
2. Kornum, L. O., and Nielsen, H. K. R., *Prog. Org. Coat.* **8,** 275 (1980).
3. Burelbach, J. P., Bankoff, S. G., and Davis, S. H., *J. Fluid Mech.* **195,** 463 (1988).
4. Dombrowski, N., and Frazer, R. P., *Philos. Trans. R. Soc. London* **247,** 101 (1954).
5. Padday, J. F., *Spec. Discuss. Faraday Soc.* **1,** 64 (1971).
6. Sharma, A., and Ruckenstein, E., *J. Colloid Interface Sci.* **137,** 443 (1990).
7. Lamb, H., "Statics," 2nd ed. Cambridge Univ. Press, Cambridge, 1916.
8. Moriarty, J. A., and Schwartz, L. W., *Journal Engrg. Math.* **26,** 81 (1992).
9. Greenspan, H. K., *J. Fluid Mech.* **84,** 125 (1978).
10. Neogi, P., and Miller, C. A., *J. Colloid Interface Sci.* **56,** 460 (1976).
11. Dussan, E. B., Rame, E., and Garoff, S., *J. Fluid Mech.* **230,** 97 (1992).
12. Moriarty, J. A., Ph.D. thesis, Dept. Mechanical Engineering, The University of Delaware, Newark, Delaware, 1991.
13. Tuck, E. O., and Vanden Broeck, J.-M., *AIChE J.* **30,** 808 (1984).